

# High Precision Measurement of the Thermal Exponent for the three-dimensional XY Universality Class

Evgeni Burovski,<sup>1</sup> Jonathan Machta,<sup>1</sup> Nikolay Prokof'ev,<sup>1,2</sup> and Boris Svistunov<sup>1,2</sup>

<sup>1</sup>*Department of Physics, University of Massachusetts, Amherst, MA 01003*

<sup>2</sup>*Russian Research Center "Kurchatov Institute", 123182 Moscow, Russia*

Simulation results are reported for critical point of the two-component  $\phi^4$  field theory. The correlation length exponent is measured to high precision with the result  $\nu = 0.6717(3)$ . This value is in agreement with recent simulation results [Campostrini *et al.*, Phys. Rev. B **63**, 214503 (2001)], and marginally agrees with the most recent space-based measurements of the superfluid transition in  $^4\text{He}$  [Lipa *et al.*, Phys. Rev. B **68**, 174518 (2003)].

PACS numbers: 64.60.Fr, 67.40.-w, 05.10.Ln

Universality at critical points is among the most beautiful and powerful ideas to emerge from statistical physics [1]. The universality hypothesis asserts that critical exponents and some other asymptotic properties of critical points are independent of microscopic details and depend on only a few properties such as the symmetry of the order parameter and spatial dimensionality. Universality permits the calculation of critical exponents for experimental systems using simplified and optimized model systems with the same symmetries. The theory of critical phenomena also predicts relationships amongst critical exponents. Among these relations are the hyperscaling relation,  $\alpha = 2 - d\nu$ , between the specific heat exponent  $\alpha$ , the correlation length exponent  $\nu$  and the dimensionality  $d$  and the Josephson relation,  $\zeta = (d - 2)\nu$  for the superfluid stiffness exponent  $\zeta$ . Improvements in experiments, theory and computer simulations have led to increasingly strict tests of universality and scaling relations. By far the most accurate experimental measurements of critical exponents are for the superfluid transition in  $^4\text{He}$ , which is in the  $O(2)$  or XY universality class. The purity of liquid Helium together with the stability of temperature control and the accuracy of specific heat measurements at low temperatures means that the limiting factor in approaching the critical singularities is the rounding due to the Earth's gravitational field. To overcome gravitational rounding, space-based microgravity experiments have been devised [3] that achieve four significant digit accuracy for the specific heat exponent  $\alpha$ . These experimental results seemingly did not agree with either analytical or numerical calculations. The experimental value itself evolved with time due to reanalysis of the data, see Refs. [3, 4, 5]. The most recent reported value being  $\nu_{\text{exp}} = 0.6709(1)$ , as inferred from the measured value of  $\alpha$  via the hyperscaling relation.

A number of recent analytical and numerical calculations were aimed at high precision determinations of  $\nu$  for the XY universality class. The vortex-loop calculations by Williams [6] yield  $\nu = 0.6717$ . Török and Hasenbusch [7] studied the two-component  $\phi^4$  model via Monte Carlo simulations. This model has a parameter that adjusts the softness of the potential constraining amplitude fluctuations of the order parameter. These authors took

advantage of this freedom to suppress the leading corrections to scaling. This study resulted in  $\nu = 0.6723(3)(8)$  (the statistical and systematic errors are given in the first and second bracket, respectively). Later the effort was advanced by Campostrini *et al.* [8] who combined Monte Carlo simulations with a high-temperature expansion to obtain  $\nu = 0.67155(27)$ , which agrees with the experimental result at the level of two standard deviations. Our study also employs a  $\phi^4$  model with fine-tuning of the Hamiltonian.

Purely analytic studies of the XY critical point include extensive treatments by Guida and Zinn-Justin, summarized in Ref. [9], which yield  $\nu = 0.6703(15)$  for the perturbative seven-loop expansion in  $d = 3$ , and  $\nu = 0.6680(35)$  for the  $\epsilon$ -expansion up to the order  $\epsilon^5$ . Jasch and Kleinert [10] developed a Borel resummation technique in the context of a strong-coupling theory which results in  $\nu = 0.6704(7)$ . The history of recent results for the correlation length exponent is given in Fig. 1.

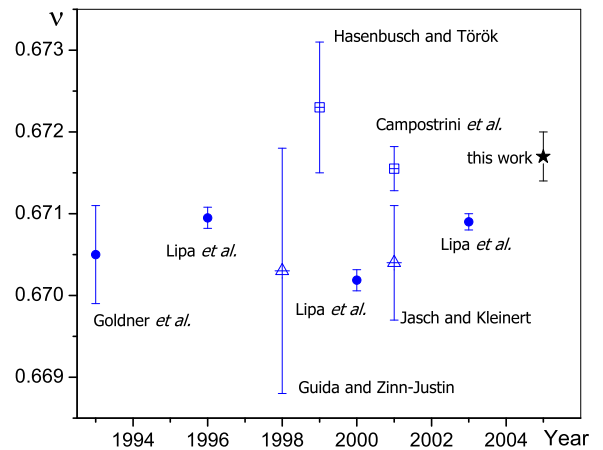


FIG. 1: Results for  $\nu$  as a function of time. Filled circles show the experimental values, open triangles depict the field-theoretic calculations, and squares show the Monte Carlo results.

The purpose of this paper is to provide high precision simulations results for the exponent  $\nu$  for the 3D XY universality class using only the Monte Carlo simulations and to compare with other theoretical, computational and experimental results.

We study a discrete 3D classical  $\phi^4$  model, defined by the Hamiltonian

$$\frac{H}{T} = -t \sum_{\langle ij \rangle} \phi_i^* \phi_j + (U/2) \sum_i |\phi_i|^4 - \mu \sum_i |\phi_i|^2, \quad (1)$$

where  $i$  and  $j$  label sites of a simple three-dimensional cubic lattice with periodic boundary conditions,  $\langle ij \rangle$  stands for the pairs of nearest neighbor sites, and  $\phi_i$  is the complex order parameter field. Since  $\phi_i$  fields are continuous and unbounded, the model (1) has only two independent parameters: by rescaling fields one can always set one parameter to unity. Henceforth, we set  $\mu = 1$ .

In order to simulate the model (1), we employ the high-temperature expansion for the partition function which transforms the configuration space into that of closed oriented loops. The latter can be efficiently sampled by the worm algorithm [11], which switches between the partition function and Green function sectors. The worm algorithm has virtually no critical slowing down and provides a direct access to the statistics of winding number fluctuations, which, in turn, define the superfluid stiffness [12]:

$$\rho_s L = \sum_{a=1}^d \langle W_a^2 \rangle / 2d. \quad (2)$$

Here  $L$  is the linear system size,  $W_a$  is the winding number in the  $a$ -th direction, and angular brackets denote averaging over the Gibbs distribution. One can also devise direct Monte Carlo estimators for the derivatives of  $\rho_s$  with respect to  $t$  and/or  $U$ , which involve cross-correlations between energy and winding numbers.

In the renormalization group (RG) framework, the finite-size scaling of the superfluid stiffness obeys the relation

$$\rho_s L = f(x) + g_\omega(x) y_\omega L^{-\omega} + \dots, \quad (3)$$

where  $x = (L/\xi)^{1/\nu}$  is the dimensionless scaling variable,  $\xi = \xi(t, U)$  is the correlation length,  $f(x)$  and  $g(x)$  are universal functions that are analytic as  $x \rightarrow 0$ ,  $y_\omega$  is the leading irrelevant scaling field, and dots represent the higher-order corrections. Field-theoretical calculations [9] yield  $\omega = 0.802(11)$  ( $\epsilon$ -expansion) and  $\omega = 0.789(11)$  ( $d = 3$  loop expansion), and the numerical analysis of Ref. [8] gives  $\omega = 0.795(9)$ .

By differentiating Eq. (3) with respect to  $t$  for  $U = U_c$  and then letting  $t \rightarrow t_c$ , one transforms (3) into

$$R'_c = AL^{1/\nu}(1 + CL^{-\omega}) + \text{higher-order terms.} \quad (4)$$

Here the derivative of  $R \equiv \rho_s L$  is taken at the critical point, and  $A$  and  $C$  are non-universal constants. Eq.

(4) is especially convenient for the numerical data analysis: the log-log plot of  $R'_c$  versus  $L$  is a straight line with the slope  $1/\nu$  for sufficiently large  $L$ . The second term adds a slight concavity or convexity to the curve for intermediate system sizes, depending on the sign of  $C$ . It is argued in Refs. [6,7] that there is little advantage in using improved models if corrections to scaling are included in the fits of MC data, and two alternative strategies of dealing with the problem are suggested. One is that MC data are fitted by discarding correction-to-scaling terms, and the possible systematic error thus introduced is estimated from the universal amplitude ratios. The other is that MC data for the critical point are used in the analysis of the high-temperature expansion series. We demonstrate below that comparable accuracy can be achieved by Monte Carlo alone, using joint fits of several improved models.

In order to locate a particular critical point, we fix some value of  $t$  and then plot  $R = \rho_s L$  as a function of  $U$  for different system sizes. The crossing of these curves in the limit of  $L \rightarrow \infty$  gives the critical point [13].

We first consider the critical point  $t_{\mathcal{A}} = -0.0795548$  and  $U_{\mathcal{A}} = 0.4101562(14)$ , which we denote by  $\mathcal{A}$ . This critical point was previously studied by Campostrini *et al.* [8] who performed an extensive and thorough search of improved models [17].

The accuracy of the critical point determination is verified by an independent Monte Carlo measurement of the first and second derivatives of  $R$ . Indeed, suppose that for a given  $U = U_c$  the value of  $t$  is off by  $\delta t = t - t_c$ . Then, expanding Eq. (3) up to  $O(\delta t^2)$  and using the data from Table I one makes sure that (i) the deviations of  $R_c$  from its universal value 0.2580(3) are consistent with  $\delta t \sim 10^{-6}$ , and (ii) the  $O(\delta t^2)$  terms are smaller than statistical errors and, thus, can be safely neglected. For example,  $R_{\mathcal{A}}(L = 48) = 0.2583(1)$  and  $R'_{\mathcal{A}}(L = 48) = 2.65 \times 10^4$ . The derivatives for  $L \neq 48$  can be computed using  $R' \propto L^{1/\nu}$  and  $R'' \propto L^{2/\nu}$ , cf. Eq. (3).

Table I lists the raw data for  $\rho'_s L$  (see below for the discussion of the dataset  $\mathcal{B}$ ). Each data point was obtained from not less than  $5 \times 10^8$  sweeps (upon equilibrating) and the accumulated data set represents approximately 18 years of CPU time. Error bars are one standard deviation and were obtained using the blocking method.

In order to magnify the fine details, we scale the numerical data with the experimental exponent,

$$q(L) = \frac{R'_c(L)L^{-1/\nu_{\text{exp}}}}{R'_c(L_0)L_0^{-1/\nu_{\text{exp}}}} \quad (5)$$

and normalize it at an arbitrarily chosen value,  $L_0 = 24$ . Figure 2 shows the data for critical point  $\mathcal{A}$ , rescaled using Eq. (5). Given the error bars, it appears that corrections-to-scaling are relevant only for  $L \lesssim 10$  and for  $L \gtrsim 10$  a straight line with the slope equal to  $1/\nu - 1/\nu_{\text{exp}}$  is a good fit, see Eqs. (4,5). A linear fit of the data for  $L \geq 10$  yields  $\nu_{\mathcal{A}} = 0.67180(7)$ , in a flagrant disagreement with the experimental value  $\nu_{\text{exp}} = 0.6709(1)$ . Our

TABLE I: Results for critical points  $\mathcal{A}$  and  $\mathcal{B}$ .

$L$	$R'_A$	$R'_B$
4	2.0329(9)	1.9906(3)
5	2.8414(5)	2.7842(7)
6	3.7316(4)	3.6583(9)
7	4.6955(5)	4.6060(5)
8	5.7289(4)	5.6215(9)
9	6.8265(7)	—
10	7.9848(9)	7.839(1)
11	9.2031(13)	—
12	10.474(2)	10.284(1)
16	16.074(4)	15.784(2)
20	22.403(4)	22.011(3)
24	29.396(7)	28.883(3)
32	45.095(13)	44.33(1)
48	82.48(3)	81.05(2)
64	—	124.40(4)
96	231.56(17)	—

value  $\nu_A$  is in agreement with the value  $\nu = 0.67155(27)$  of Ref. [8] within the combined error bars. However, our new data for critical point  $\mathcal{A}$  are more accurate and yield a smaller error bar. We have also studied a version of the improved link-current model [15], which belongs to the same universality class. When these data were fit by a straight line, we observed even greater discrepancies with  $\nu_{\text{exp}}$ .

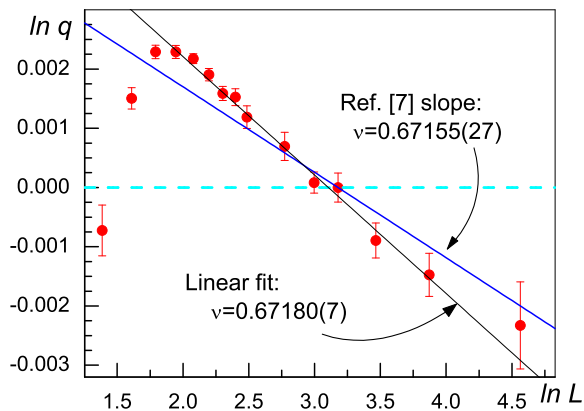


FIG. 2: The derivative of  $R_A$  rescaled via Eq. (5). Dashed horizontal line corresponds to  $\nu = \nu_{\text{exp}}$ . See the text for discussion.

To understand the apparent disagreement with experiment, we performed a series of simulations for critical points in the vicinity of the critical point  $\mathcal{A}$  to map out the region where  $C = C(t_c, U_c)$  is small. We then carried out a large-scale simulation of one of the critical points,  $\mathcal{B}$ , characterized by  $t_B = -0.07142822$  and  $U_B = 0.3605750(8)$ . Table I shows the raw data

for this critical point ( $R_B(L = 48) = 0.2577(1)$  and  $R_B''(L = 48) = 1.27 \times 10^4$ ). A naïve linear fit of the dataset  $\mathcal{B}$  for  $L \geq 10$  yields  $\nu_B = 0.67142(5)$ , which is inconsistent with  $\nu_A$ . Critical points  $\mathcal{A}$  and  $\mathcal{B}$  are equally legitimate and we are left in a quandary as to whether to reject universality or to consider a more careful analysis of the data. We choose the later course.

It becomes obvious that there is no easy way to improve the accuracy of the critical exponent calculations by ignoring corrections to scaling, even when they appear very small. To reconcile the results for the datasets  $\mathcal{A}$  and  $\mathcal{B}$  one *must* include the subleading corrections in the fits. If this is done for each dataset separately, it leads to a large increase (almost by an order of magnitude) in the uncertainty of the fits, as has been noted in Ref. [8]. Tighter error bars can be obtained performing a *joint* fit of two datasets. More specifically, we perform a 6-parameter fit according to

$$\ln q \sim B + \left( \frac{1}{\nu} - \frac{1}{\nu_{\text{exp}}} \right) \ln(L/L_0) + CL^{-\omega}, \quad (6)$$

as follows from Eqs. (4) and (5) for  $C \ll 1$ . The fitting parameter  $B$  is introduced in order to undo the artificial normalization  $q(L = L_0) = 1$ . Here each critical point has its own amplitudes  $B$  and  $C$ , while the universal exponents  $\nu$  and  $\omega$  are shared between the datasets, which yields six fitting parameters.

We performed the joint fit according to Eq. (6) via stochastic minimization of  $\chi$ -square. We constrained the exponent  $\omega$  to within  $\pm 0.03$  around 0.795, which is the  $3\sigma$  interval of the established value [8]. We also discarded small system sizes  $L < L_{\text{cutoff}} = 10$ . The optimization procedure yields  $\nu = 0.6717(3)$  at the confidence level [14]  $\text{CL} \approx 0.43$ . This value is consistent with the result of Ref. [8], and also marginally agrees with the experimental value [3]. The fit is depicted in Fig. 3 and yields

$$\begin{cases} C_A = (1.5 \pm 0.5) \times 10^{-3}, \\ C_B = (-1.0 \pm 0.3) \times 10^{-2}, \\ \nu = 0.6717(3). \end{cases} \quad (7)$$

Note that the dataset  $\mathcal{A}$  points are exactly the same as in Fig. 2 and a slight curvature is visible in Fig. 3 which is unaccounted for in Fig. 2. It is also worth noting that the best-fit value of  $\omega$  is  $\omega = 0.81(1)$  which is consistent with the field-theoretic estimates [9]. The error bars in Eq. 7 reflect both stochastic and systematic uncertainties, the latter being estimated via changing the  $L_{\text{cutoff}}$  for the dataset  $\mathcal{A}$  and/or  $\mathcal{B}$ .

One might question the relevance of higher order corrections to scaling omitted from Eq. (3). The next order correction is proportional to the square of the leading irrelevant field,  $\propto C^2 L^{-2\omega}$ , i.e. it contains the square of the already small amplitude  $C$  [16]. A sizable cumulative amplitude of higher-order corrections would exhibit itself for the smallest system sizes,  $L \lesssim 12$ . In the contrary, the scaling curves for both models under consideration have

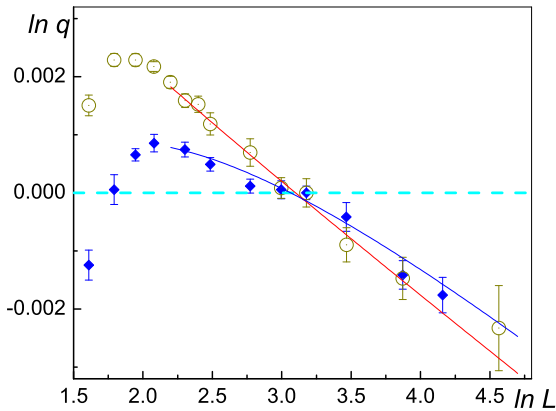


FIG. 3: Data from Table I rescaled via Eq. (5). Circles: dataset  $\mathcal{A}$ , diamonds: dataset  $\mathcal{B}$ . Dashed horizontal line corresponds to  $\nu = \nu_{\text{exp}}$ . Solid lines are the results of the joint fit of both datasets (see the text for explanation). Note the scale of the vertical axis.

overall vertical scale on the order of  $10^{-3}$  for system sizes as small as  $L = 4$ .

The apparent controversy concerning the 3D XY universality class is resolved. Our calculated value of  $\nu = 0.6717(3)$  is in agreement with the results of recent simulation [8], and also marginally agrees with the best experimental value  $\nu_{\text{exp}} = 0.6709(1)$ , deduced from  $\alpha$  via hyperscaling relation. We demonstrate that one has to be careful when working with improved models and always include corrections to scaling into the fit, even when the data set allows a good linear fit. The fourth-digit accuracy in critical exponents can be reached by simultaneously fitting more than one critical point.

We acknowledge support from NASA under Grant NAG-32870.

- 
- [1] M.E. Fisher, in *Lecture Notes in Physics* **186**, Springer-Verlag, 1983.
  - [2] L.S. Goldner, N. Mulders, G. Ahlers, J. Low Temp. Phys. **93**, 131 (1993).
  - [3] J.A. Lipa, J.A. Nissen, D.A. Stricker, D.R. Swanson, and T.C.P. Chui, Phys. Rev. B **68**, 174518 (2003).
  - [4] J.A. Lipa, D.R. Swanson, J.A. Nissen, Z.K. Geng, P.R. Williamson, D.A. Stricker, T.C.P. Chui, U.E. Israelsson, and M. Larson, Phys. Rev. Lett. **84**, 4894 (2000).
  - [5] J.A. Lipa, D.R. Swanson, J.A. Nissen, T.C.P. Chui, and U.E. Israelsson, Phys. Rev. Lett. **76**, 944 (1996).
  - [6] G. A. Williams, Phys. Rev. Lett. **82**, 1201 (1999).
  - [7] M. Hasenbusch, T. Török, J.Phys. A: Math. Gen, **32** 6361 (1999).
  - [8] M. Campostrini, M. Hasenbusch, A. Pelissetto, P. Rossi, and E. Vicari, Phys. Rev. B **63**, 214503 (2001)
  - [9] R. Guida and J. Zinn-Justin, J. Phys. A **31**, 8103 (1998).
  - [10] F. Jasch, H. Kleinert, J. Math. Phys. **42**, 52 (2001).
  - [11] N.V. Prokof'ev and B.V. Svistunov, Phys. Rev. Lett. **87**, 160601 (2001)
  - [12] E.L. Pollock and D.M. Ceperley, Phys. Rev. B **36**, 8343 (1987).
  - [13] K. Binder, Phys. Rev. Lett. **47**, 693 (1981).
  - [14] W.H. Press, S.A. Teukolsky, W.T. Vetterling, and B.P. Flannery, *Numerical Recipes in C*, 2nd ed, Cambridge, 1992
  - [15] M. Wallin, E.S. Sørensen, S.M. Girvin, and A.P. Young, Phys. Rev. B **49**, 12115 (1994).
  - [16] M. Hasenbusch, J. Phys. A: Math. Gen. **32**, 4851 (1999).
  - [17] the notation of Ref. [8] is related to our's via  $t = \beta/2(2\lambda - 1)$  and  $U = 2\lambda/(2\lambda - 1)$ .